Colloid Polym Sci (2005) 284: 322–326
DOI 10.1007/s00396-005-1371-9

SHORT COMMUNICATION

Wei Zeng
Jijun Wang
Zoujun Feng
Jin-Yong Dong
Shouke Yan

Morphologies of long chain branched isotactic polypropylene crystallized from melt

Received: 4 February 2005
Accepted: 14 June 2005
Published online: 15 September 2005

W. Zeng · J. Wang · S. Yan (✉)
State Key Laboratory of Polymer Physics and Chemistry, Joint Laboratory of Polymer Science and Materials,
Institute of Chemistry,
The Chinese Academy of Sciences,
Beijing 100080, China
E-mail: skyan@iccas.ac.cn
Tel.: +86-10-82618476
Fax: +86-10-82618476

Z. Feng · J.-Y. Dong
CAS Key Laboratory of Plastic Engineering,
Joint Laboratory of Polymer Science and Materials,
Institute of Chemistry,
The Chinese Academy of Sciences,
Beijing 100080, China

Abstract The crystallization behavior and resulting crystalline morphologies of long chain branched isotactic polypropylene (LCBPP) under different conditions were studied by means of differential scanning calorimetry and transmission electron microscopy combined with electron diffraction. The results indicate that the crystallization of LCBPP during fast cooling process, or at lower crystallization temperature, leads to the formation of mainly edge-on lamellar structures. The LCBPP exhibits also the wide angle lamellar branching frequently observed for linear isotactic polypropylene. Crystallizing LCBPP in temperature range of 110∼140 °C results in the formation of both edge-on and flat-on crystals, which coexist side by side with the content of flat-on crystals increases with increasing crystallization temperature. At high crystallization temperature, e.g. 145 °C, flat-on crystals with chain axis aligned perpendicular to the film plane are the only observed morphology. Moreover, the crystals of LCBPP grow slower than its linear counterpart and the crystal growth rates of both linear and long branched PPs are temperature dependent.

Keywords LCBPP · Crystallization · Morphology

Introduction

The crystallization kinetics and crystalline morphologies of isotactic polypropylene (iPP) have been extremely active research topics for more than 40 years [1–10]. It was well documented that iPP exhibits pronounced polymorphisms and morphologies depending on the molecular weight, thermal treatments, and mechanical handling. At least three different polymorphs, designated as monoclinic α, hexagonal β and triclinic γ, have been reported in the literatures [11–15]. Among these three forms, the monoclinic α-form is the thermodynamically most stable and commonly observed one of iPP crystallized from both melt and solution [2–4]. It can form a cross-hatched structure, which has not be seen in other semicrystalline polymers, stemming from characteristic lamellar branching. The characteristic lamellar branching was explained in terms of homoepitaxy of the daughter lamellae on mother lamellae with their chain directions 80° apart from each other [3, 4, 7, 9].

It should be pointed out that iPP produced either by Ziegler-Natta catalyst or by metallocene catalyst exhibits normally a linear structure. The linear iPP is one of the most intriguing thermoplastic polymers because of its desirable physical properties, such as high tensile strength, stiffness, chemical resistance and thermal stability [16]. Its application is, however, limited in blow molding, thermoforming, and foaming due to its poor process ability based on relatively low melt strength [17]. Therefore, great effort has been made in the past few

decades to improve the melt strength of iPP. Among them, the most widely adopted way for modifying iPP is either to blend it with other polymers or to copolymerize the propene with other component. Recently, it was found that introducing long chain branches into linear polymer provides an efficient way for enhancing its melt strength [18, 19]. As a consequence, much attention was paid to produce long chain branched polypropylene (LCBPP) [20–23]. At the same time, increasing interesting was seen in characterizing the novel synthesized LCBPP. Up to now, a number of research work has been carried out in this field, including molecular weight measurement by GPC [23, 24], chemical structure characterization using NMR [23, 25], thermoanalysis via DSC [25], crystalline structure determination with X-ray scattering [24], and so on. However, the crystalline morphology of LCBPP was rarely concerned so far.

In this paper, under the basic knowledge of iPP, we report our recent work on the crystalline structure and morphology of a newly synthesized LCBPP by transmission electron microscopy (TEM) combined with electron diffraction.

Experimental

Materials

The LCBPP used in this work, with melt flow index (MFI) of 2.1 g/10 min, $M_w \approx 3.96 \times 10^5$, and melting temperature(T_m) of 150 °C, was kindly provided by Prof. Dong.

Sample preparation and measurements

Ultrathin LCBPP films suitable for TEM study were prepared by spin coating a 0.1 wt% LCBPP solution in xylene on carbon coated freshly cleaved mica sheets with a rotation speed of 2,000 rpm. The spin coated ultrathin LCBPP films were heat-treated at 200 °C for 5 min, and subsequently cooled either direct to a desired temperature for isothermal crystallization or with different rates to room temperature. The isothermal crystallization temperature was set in the range of 120–150 °C. The thermal treatment was performed on a LTS350 hot stage with accuracy of ±0.1 °C under the nitrogen atmosphere. The thus prepared thin films were floated on the surface of distilled water, and then mounted onto 400-mesh TEM grids for TEM observation.

For TEM observation, a JEM-100CX TEM operated at 100 kV was used in this study. Bright-field (BF) phase contrast electron micrographs were obtained by defocus of the objective lens [26, 27]. In order to minimize radiation damage of the polymer samples caused by the electron beam, focusing of the sample was carried out on one area, the specimen film was then translated to its adjacent undamaged area and the image was recorded immediately.

Results and discussion

Figure 1 shows the phase contrast BF electron micrograph and its corresponding electron diffraction pattern of LCBPP thin films melt-crystallized during the cooling process at a rate of 30 °C/min. In the phase contrast BF image, the bright areas represent the lower mean inner potential amorphous regions, while the gray areas correlate to the high-density crystalline lamellar regions. From Fig. 1a, it can be clearly seen that cooling the LCBPP melt at a rate of 30 °C/min leads to the formation of lamellar structure. The lamellar structure is, however, somewhat different from its linear counterpart. The characteristic lamellar branching with the mother and daughter lamellae 80° apart is not so pronounced as the linear iPP [28, 29]. This has further been confirmed by the corresponding electron diffraction, see Fig. 1b. The appearance of the diffraction rings unambiguously indicates the random orientation of the LCBPP crystalline lamellae. There exist, nevertheless, many lamellar bundles, as indicated by the white circles, which look like bundles of plant stems enlaced by strips. The enlacing strips, i.e. the central transverse lamellae, are

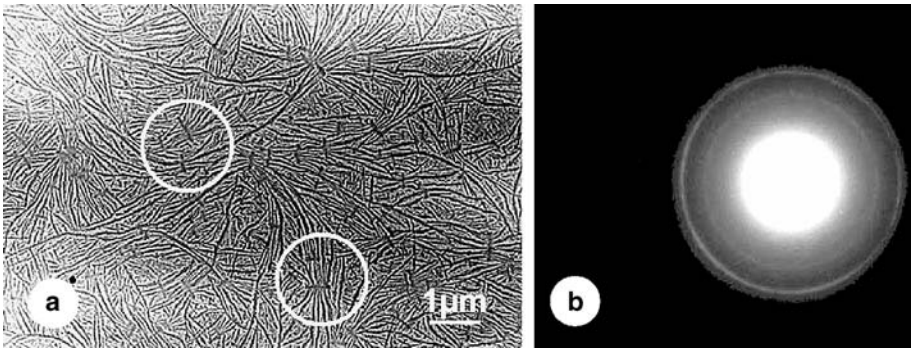

Fig. 1 Phase contrast BF electron micrograph and its corresponding electron diffraction pattern of LCBPP thin films crystallized during the cooling process at a rate of 30 °C/min

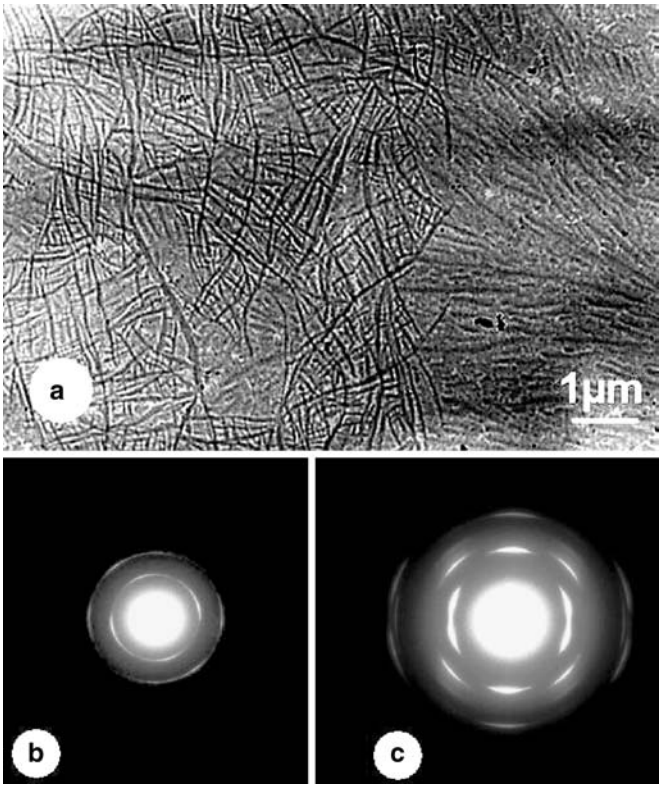

Fig. 2 Phase contrast BF electron micrograph and its corresponding electron diffraction patterns of LCBPP thin films crystallized during the cooling process at a rate of 20 °C/min

thicker than the bundle lamellae. This may imply that the central transverse lamellae form first and initiate the growth of the bundle lamellae. The fact that the bundle lamellae are about 80° apart from the central transverse lamellae leads to the conclusion that homoepitaxy takes place occasionally.

The supermolecular structure of LCBPP depends strongly on the cooling condition of its melt. For example, when cooling the LCBPP melt with a rate of 20 °C/min, as seen in Fig. 2a, two kinds of structures have been observed. The corresponding electron diffraction patterns, parts b and c of Fig. 2, indicate that the left part of Fig. 2a exhibits an edge-on lamellar structure with molecular chains oriented in the film plane, while the right part of Fig. 2a corresponding to a flat-on structure with crystals viewed along the *c*-axis. The edge-on and flat-on crystals coexist side by side even in the same spherulite. Moreover, with careful inspection, it can be recognized that the edge-on lamellae presented in the left part of Fig. 2a is somewhat different form that shown in Fig. 1a. In Fig. 2a, a cross-hatched structure can be evidently observed. The corresponding electron diffraction pattern, see Fig. 2b, confirms the occurrence of homoepitaxy with the parallel packing of *a*- and *c*-axes of daughter lamellae along the *c* and *a* axes of the mother lamellae, respectively [28, 29]. This kind of structure has frequently been observed and well explained in the literatures for linear polypropylene [3, 4, 7, 9].

Further decreasing of the cooling rate leads to the amount increase of flat-on crystals. Figure 3 shows the BF electron micrographs and their corresponding electron diffraction patterns (insets of Fig. 3) of the LCBPP crystallized during the cooling process with the cooling rate of 5 °C/min. Now the edge-on and flat-on crystals still coexist side by side. The edge-on crystalline region, Fig. 3a, has close resemblance with that shown in the left part of Fig. 2a, indicating the formation of a cross-hatched lamellar structure. The flat-on crystalline region is, however, different from the right part of Fig. 2a. As shown in Fig. 3b, the top surface of the flat-on crystal formed under present condition is much smoother than that formed at higher cooling rate. Moreover, the electron diffraction pattern, inset of Fig. 3b, shows well-defined sharper reflection spots, which is somewhat closer to that of single crystals.

The above-observed morphological changes with cooling rate are actually related to the crystallization temperature. DSC measurement was performed to estimate the exact crystallization temperature in those cooling processes. As shown in Fig. 4, the crystallization temperature increases apparently with the decrease of the cooling rate. Nevertheless, the highest crystallization temperature of the aforementioned cooling processes is ca. 112 °C. To check the crystalline morphology of LCBPP crystallized at even higher temperatures, isothermal crystallization at different temperatures was conducted.

Figure 5 shows the BF electron micrographs of LCBPP crystallized isothermally at 130, 140, and 145 °C, respectively. From Fig. 5a, it can be found that, crystallizing isothermally at 130 °C, the LCBPP shows predominately the flat-on lamellar structure. The flat-on crystals packed closely together forming narrow lath-like crystals with their center parts having darker contrast. This may imply that the center part of the lath-like crystal is thicker than its edge regions. There do exist some edge-on lamellae, as indicated by the white arrows in Fig. 5a, which dispersed between the flat-on lath-like crystals. The edge-on lamellae are principally perpendicular to the boundary line of the lath-like crystal. With close inspection, one can find some short edge-on lamellae arranging approximately in the direction parallel to the boundary line of the lath-like crystals. This part of the lamellae is induced by the transverse edge-on lamellae through homoepitaxy.

With increasing crystallization temperature, the lath-like crystals become wider and wider. For example, crystallizing the LCBPP at 140 °C leads to the formation of lath-like crystals with width of micrometer scale, see Fig. 5b. Moreover, now a thin flat-on crystal layer with

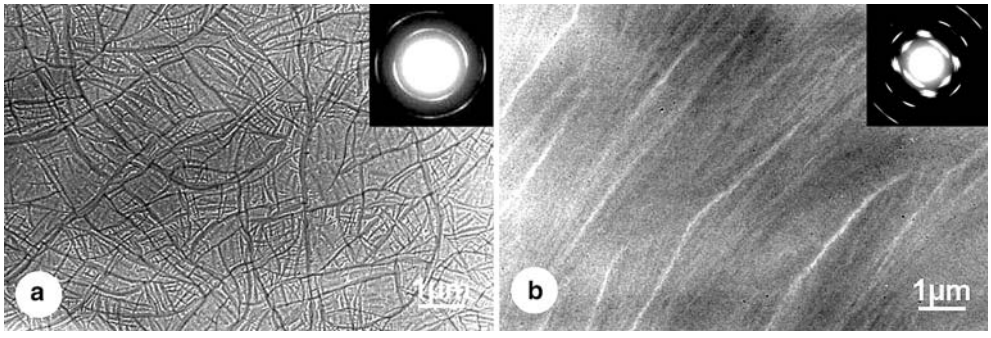

Fig. 3 Bright-field electron micrographs and their corresponding electron diffraction patterns (*insets*) of the LCBPP crystallized during the cooling process at a cooling rate of 5 °C/min

weaker contrast can be clearly seen in the edges of the crystalline laths, as indicated by a white arrow in Fig. 5b. This may be associated with the material depletion caused by insufficient material diffusion. It should be pointed out that there exist still some edge-on crystalline regions, which stand directly by the thin flat-on crystals. Also the characteristic wide angle lamellar branching has been clearly observed in these areas. With further increase of the crystallization temperature, e.g. 145 °C, only lath-like crystals with very smooth surface have been observed. The corresponding electron diffraction pattern, inset of Fig. 5c, shows sharp and well defined (*hk0*) reflection spots in its α-modification. Figure 5c further indicates that the crystallographic *a*-axis is parallel to the length direction of the LCBPP lath crystals. In other words, similar to the linear PP, the *a*-axis is also the fastest growth direction of LCBPP crystals.

From the above results, it is concluded that the long chain branch, in same length order of main chain, has little influence on the structure and morphology of PP. There may be, however, some influence on the crystallization kinetics. Therefore, linear spherulite growth rates of LCBPP under different temperatures were measured by in situ optical microscopy observations. Figure 6 shows the plot of LCBPP spherulite growth

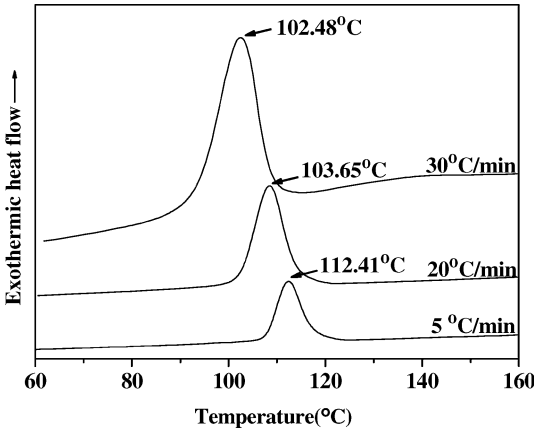

Fig. 4 DSC cooling scans of LCBPP at different cooling rates

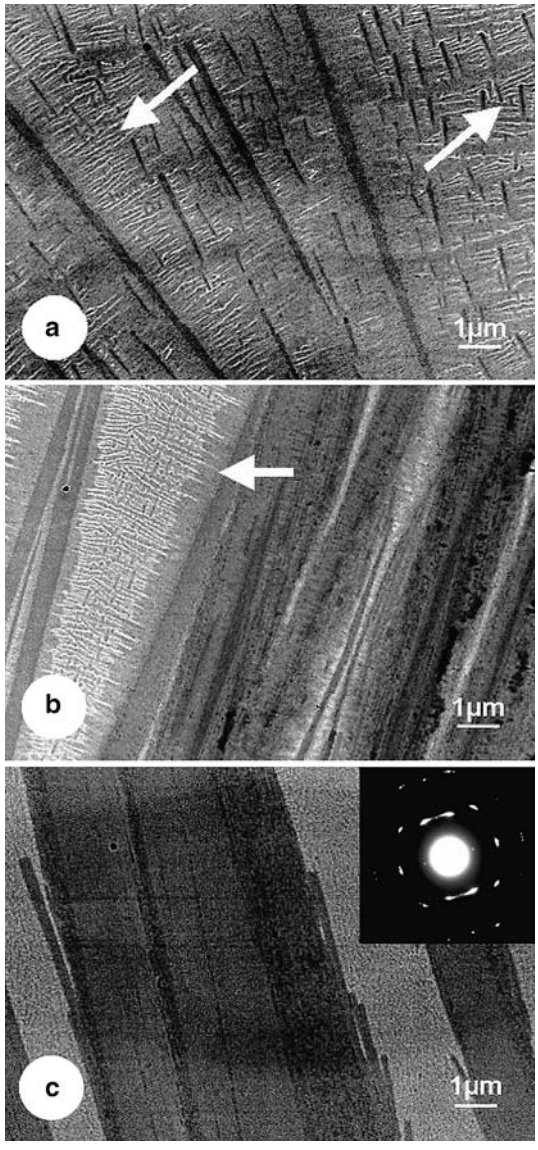

Fig. 5 Bright-field electron images of the LCBPP crystallized isothermally at **a** 130, **b** 140, and **c** 145 °C. The *inset* of Fig. 5c shows its corresponding electron diffraction pattern

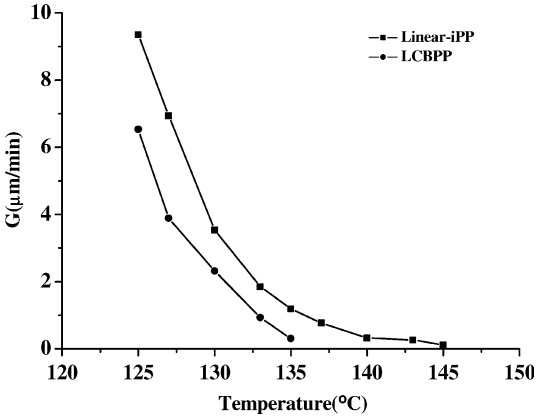

Fig. 6 The plots of linear crystal growth rates of LCBPP and linear PP via temperature

rates via temperature. For direct comparison, the growth rate via temperature plot of a linear PP with $T_m \approx 151$ °C and MFI of 7.0 g/10 min synthesized by Dong's group is also presented. From Fig. 6, it can be clearly seen that the crystal growth rates of both linear and long chain branched PPs decrease with increasing temperature. Furthermore, the growth of linear PP crystals is always faster than its long chain branched counterpart. This may be result from the reduction of chain mobility of LCBPP caused by long side chains as can be judged from small MFI value.

Conclusions

In summary, the crystallization behavior and the resulting crystalline morphology of LCBPP were studied. The results indicate that the morphology of it depends strongly upon the crystallization condition. Crystallization of the LCBPP during the fast cooling process, or at lower crystallization temperature, leads to the formation of mainly edge-on lamellar structure. The characteristic wide angle lamellar branching, frequently observed for linear iPP, is also observed for LCBPP. Crystallizing LCBPP at moderate temperature range results in the formation of both edge-on and flat-on LCBPP crystals, which coexist side by side even in the same spherulite. The content of flat-on crystals increases with increasing crystallization temperature. At high crystallization temperature, e.g. 145 °C, flat-on crystals with chain axis aligned perpendicular to the film plane are the solely observed morphology. This is quite similar to the linear PP. The LCBPP crystals grow, however, slower than their linear counterparts and the crystal growth rates of both PPs are temperature dependent.

Acknowledgements The financial support of the CAS (No. KJCX2-SW-H07), the 973 program (No.2003CB615600), and National Natural Science Foundation of China is gratefully acknowledged.

References

1. Padden FJ Jr, Keith HD (1959) J Appl Phys 30:1479
2. Padden FJ Jr, Keith HD (1966) J Appl Phys 37:4013
3. Padden FJ Jr, Keith HD (1973) J Appl Phys 44:1217
4. Khoury F (1966) J Res Natl Bur Stand A70:29
5. Binsbergen FL, DeLange BGM (1968) Polymer 9:23
6. Lovinger AJ, Chua JO, Gryte CC (1977) J Polym Sci Polym Phys Edn 15:641
7. Lovinger AJ (1983) J Polym Sci Polym Phys Edn 21:97
8. Norton DR, Keller A (1985) Polymer 26:704
9. Bassett DC, Vaughan AS (1985) Polymer 26:717
10. Lotz B (2002) J Macromol Sci Phys B41:685
11. Turner-Jones A, Cobbold AJ (1968) J Polym Sci B6:539
12. Morrow DR, Newman BA (1968) J Appl Phys 39:4944
13. Bruckner S, Meille SV (1989) Nature (London) 340:455
14. Meille SV, Bruckner S, Porzio W (1990) Macromolecules 23:4114
15. Lotz B, Graff S, Straupe C, Wittmann JC (1991) Polymer 32:2902
16. Platz C (2001) In: Presented at the International Conference on Polyolefins, Houston, TX
17. McDonald JN (1989) Thermoforming. In: Encyclopedia of polymer science and engineering, vol 16. Wiley, New York, pp 807
18. Roovers J (1991) Macromolecules 24:5895
19. Kokko E, Malmberg A, Lehmus P, Lofgern B, Seppala JV (2000) J Polym Sci Part A Polym Chem 38:376
20. Lu B, Chung TC (1999) Macromolecules 32:8678
21. Weng W, Marke EJ, Dekmezian AH (2000) Macromol Rapid Commun 21:103
22. Weng W, Marke EJ, Dekmezian AH (2001) Macromol Rapid Commun 22:1488
23. Weng W, Hu W, Dekmezian AH, Ruff CJ (2002) Macromolecules 35:3838
24. Agarwal PK, Somani RH, Weng WQ, Mehta A, Yang L, Ran SF, Liu LZ, Hsiao BS (2003) Macromolecules 36:5226
25. Ye ZB, Zhu SP (2003) J Polym Sci Part A Polym Chem 41:1152
26. Petermann J, Gleiter H (1975) Philos Mag 31:929
27. Miles JM, Petermann J (1979) J Macromol Sci Phys B 16:243
28. Lotz B, Wittmann JC (1986) J Polym Sci Part B Polym Phys 24:1541
29. Lotz B, Wittmann JC, Lovinger AJ (1996) Polymer 37:4979